Innovations in applied physics

Izvestiya Vysshikh Uchebnykh Zavedeniy. Applied Nonlinear Dynamics. 2024;32(3)

Article DOI: 10.18500/0869-6632-003103

Spectral approach with iterative clarification of a radiation boundary conditions for modeling of quasimodes of a gyrotrons open cavities

A. G. Rozhnev[1,2]✉, *M. M. Melnikova*[3,1], *N. M. Ryskin*[1,2]

[1]Saratov Branch of Kotelnikov Institute of Radioengineering and Electronics, Russia
[2]Saratov State University, Russia
[3]FRC A. V. Gaponov-Grekhov Institute of Applied Physics of the RAS, Nizhny Novgorod, Russia
E-mail: ✉RozhnevAG@mail.ru, Mafashu@mail.ru, RyskinNM@gmail.com
Received 30.11.2023, accepted 25.12.2023, available online 10.04.2024, published 31.05.2024

Abstract. *Purpose.* The article presents a new method for numerical simulation of quasi-eigenmode oscillations in open resonators of gyrotrons — powerful vacuum generators of electromagnetic waves in the millimeter and submillimeter ranges. The gyrotron cavity has the shape of a weakly inhomogeneous hollow circular metal waveguide. *Methods.* The proposed approach uses the inhomogeneous string equation with radiation boundary conditions to formulate a nonlinear spectral boundary value problem describing oscillations in a resonator, neglecting the couplings of waves with different radial indices. By linearizing with respect to frequency the radiation boundary conditions, the boundary value problem is reduced to a linear boundary value problem. To discretize this boundary value problem, the finite difference method is used and a linear generalized matrix eigenvalue problem is formulated. This problem is solved by the Arnoldi method with eigenvalues calculation in a shift-invert mode. An iterative algorithm is proposed that makes it possible to sequentially calculate a given number of frequencies and quality factors of quasi-eigenmodes of oscillations. *Results.* The computer program was developed written in the Wolfram Language and Fortran using the algorithms proposed in the work. The results of test calculations for real gyrotron resonators are presented, which demonstrate the high accuracy of the obtained values of frequencies, quality factors and field distributions of quasi-eigenmode oscillations in the studied resonators. *Conclusion.* The methods, algorithms and created program proposed in the article can significantly facilitate the process of developing gyrotrons intended for various practical applications and operating in new frequency ranges. The method of iterative refinement of boundary conditions can be generalized to the case of equations of the linear theory of a gyrotron and used to develop new methods for analyzing the starting conditions for the soft self-excitation in gyrotrons — generators.

Keywords: gyrotron, open cavity, high order axial modes, radiation boundary condition, finite difference method, generalized matrix eigenvalue problem, Arnoldi method.

Acknowledgements. This study was performed within the framework of a state order to the Kotelnikov Institute of Radio Engineering and Electronics of the Russian Academy of Sciences.

For citation: Rozhnev AG, Melnikova MM, Ryskin NM. Spectral approach with iterative clarification of a radiation boundary conditions for modeling of quasimodes of a gyrotrons open cavities. Izvestiya VUZ. Applied Nonlinear Dynamics. 2024;32(3):305–331. DOI: 10.18500/0869-6632-003103

Introduction

The gyrotron is a source of powerful electromagnetic radiation in the microwave, subterahertz and terahertz frequency ranges [1–3]. It is widely used in various fields of science and technology, such as plasma heating and diagnostics in fusion plants [4, 5], radio spectroscopy [6–11], medicine [12–15], technological processes [16–19], communication systems [20] and other applications.

Recently, various applications of gyrotrons have been of particular interest, for which it is necessary to comply with special requirements imposed on the distribution of the field of the working mode along the interaction space, which is determined by the shape of the resonator. For example, in gyrotrons for thermonuclear reactors with a megawatt output power level, resonators with a small length-to-radius ratio are required, as well as with ultra-small reflections of the output signal from the output device back to the area of interaction. The fulfillment of these conditions is achieved due to a multi-stage or superalloy transition from the interaction region to the output horn with a controlled law of variation of the resonator radius along its axis.

In gyrotrons being developed for spectroscopic installations operating on the effect of nuclear magnetic resonance with dynamic polarization of nuclei, it should be possible to quickly adjust the generation frequency in the range of 1-2 GHz [11] and high frequency stability during tens of hours of continuous operation. One of the ways to adjust the frequency is to change the magnetic field. At the same time, the conditions of synchronism of the oncoming wave in the resonator with the cyclotron wave in the electron beam change, and, as a result, the generation frequency changes. The field distribution along the system is rearranged in such a way that the interaction mainly occurs with various longitudinal modes of the resonator. The possibility of excitation of high-order longitudinal modes is provided by choosing a suitable resonator profile.

Finally, another important area of gyrotron development is the creation of sources of powerful radiation in the terahertz range at frequencies from several hundred GHz to 1.2–1.5THz [21–25]. To do this, the interaction at the higher harmonics of the cyclotron frequency (second and third) is used. The main problem in this case is the suppression of parasitic generation at the fundamental harmonic of the cyclotron frequency. The necessary mode selection is also achieved by selecting the resonator profile.

In the research and development of modern gyrotrons, computer modeling is the most important tool, based on which contains a set of theoretical approaches and models of various levels of complexity — from simple one-dimensional models for calculating the properties of vibrations in a gyrotron resonator without a beam to direct numerical modeling of the interaction of the beam with the electromagnetic field of the resonator using a self-consistent solution of Maxwell's equations and equations of electron motion in 2.5D or a full three-dimensional formulation [26–29]. The literature presents both computer codes designed to solve each of these particular problems, and software packages consisting of modules in which all or most of the techniques used at different stages of gyrotron design are implemented [30–38].

One of the most important components of such modeling is the calculation of the properties of a gyrotron resonator without an electron beam. These properties include the oscillation frequencies in the resonator, their ohmic and diffraction Q-values, as well as the distribution of the electromagnetic field components along the resonator. The resonator used in the classical gyrotron design is a weakly homogeneous hollow round metal waveguide, the radius of which varies slightly along the longitudinal axis. On both sides, a segment of an inhomogeneous waveguide is loaded onto horns, one of which narrows at the cannon end, and the other expands at the collector end of the system (see Fig. 1). In general, such a structure is an open electrodynamic resonator [2,39–41], in which there may be high-frequency electromagnetic oscillations arising due to wave reflections

from transitions of a homogeneous section of the waveguide into horns. These oscillations in open electrodynamic structures are called quasi-spatial, or complex [39], since they differ in some of their properties from their own types of oscillations in closed hollow metal resonators.

When developing gyrotrons, in order to determine the optimal shape of the resonator, it is necessary to repeatedly solve the problem of calculating the properties of oscillations, setting various dependences of the radius of the inhomogeneous waveguide on the longitudinal coordinate. The simplest and at the same time effective model for calculating oscillations in an open gyrotron cavity is based on the use of the one-dimensional equation of an inhomogeneous string together with radiation boundary conditions (RBC) at its ends [40]. In this case, the function $F(z)$, with respect to which the boundary value problem is formulated, describes the distribution of the complex amplitude of the field along the axis of the resonator. For TE_{mn} modes, it is the complex amplitude of H_z-components of the electromagnetic field, and for TM_{mn}-modes — the complex amplitude of E_z-components of the field. Here m and n are the transverse azimuthal and radial mode indices. Classical gyrotrons use TE_{mn}-types of vibrations, so only they will be considered further. The simplicity of the model based on the inhomogeneous string equation is explained by the fact that it does not take into account small connections between the main mode and modes with other values of the radial index n.

The field distribution $F(z)$ in the main part of the resonator has a characteristic standing wave appearance with a different number of field variations along the system. Depending on the number of variations, fluctuations occur with different frequencies and Q-values. The number of variations is denoted by the integer q, and oscillations with different q are called different longitudinal modes of the open resonator. In general, these modes are designated as TE_{mnq}.

In the area of the output horn, the field has the form of a wave escaping from the resonator, which carries away part of the energy of the electromagnetic field into the output path. Due to this, the oscillations in the resonator have a finite Q-factor even in conditions when the walls of the resonator are made of an ideally conductive material. In this case, this Q factor is called diffraction and is denoted by Q_d. If losses due to the finite conductivity of the wall material are additionally taken into account, ohmic losses are added to the diffraction losses, and if both types of losses are small, the total quality factor is determined using the formula $Q_t = (Q_d Q_o)/(Q_d + Q_o)$, where $Q_t$and Q_o — total and ohmic Q-values of oscillations, respectively.

Despite the apparent simplicity of the approach based on solving the inhomogeneous string equation, a number of problems arise in its numerical implementation. Although the equation itself is linear, the numerical solution of the complete boundary value problem describing free oscillations in the resonator requires the use of iterative methods, since the complex oscillation frequency, acting in this case as a spectral parameter, enters the RBC in a nonlinear way. To find all solutions in a given area of the complex frequency plane, it is necessary to involve additional theoretical or empirical considerations to determine the number of modes and set the initial

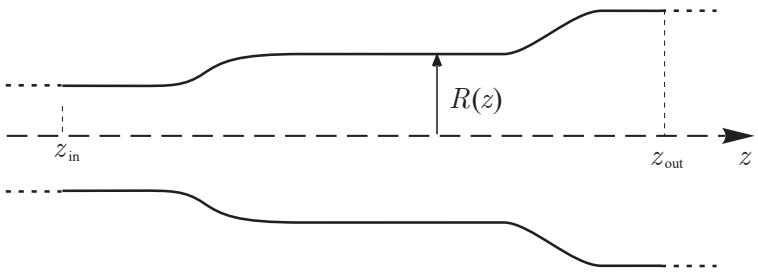

Fig 1. Gyrotron cavity as weakly irregular hollow metallic waveguide

approximations necessary to start the iteration process.

This problem is especially acute when analyzing resonators with ultra-low diffraction Q-factor used in high-power gyrotrons of the subterahertz and terahertz ranges, since in this case the regularity of the arrangement of frequencies of different modes on the complex plane is violated. When calculating a large number of longitudinal modes in the studied part of the spectrum, additional non-physical solutions (with low Q-values) may appear, in which the field amplitude increases sharply in the area of the output horn. The frequencies and Q-values of these modes turn out to be close to the corresponding values for higher longitudinal modes localized in the central part of the resonator. In the presence of non-physical modes, it is difficult to set reasonable initial approximations for a priori reasons and they have to be found practically «manually».

Most often, the [46] targeting method is used to solve the above boundary value problem [30–38]. In other cases, instead of searching for eigenvalues (ES), the problem of exciting the resonator with an external harmonic signal is solved, after which the values of frequencies and Q-values are found from the analysis of the calculated resonance curve [42–45].

In the work [46], a new approach to the search for complex oscillation frequencies in the gyrotron resonator, called spectral, was proposed. Its essence lies in the fact that differential equations, together with boundary conditions, are reduced by one of the difference methods (finite differences or finite elements) to a generalized matrix eigenvalue problem, in which the normalized detuning of the oscillation frequency from the critical frequency of the operating mode acts as a spectral parameter. In [46], this technique is used to calculate self-excitation conditions in the linear mode of operation of a gyrotron, but it is obvious that the same approach in a simpler version can be used to search for complex oscillation frequencies in a gyrotron resonator without a beam. However, when using the spectral approach in the form proposed in [46], it turns out that some elements of the matrices of the generalized matrix problem themselves depend on the spectral parameter, so in general it turns out to be nonlinear and the same difficulties arise when solving it as in the targeting method — the need to specify initial approximations for each from the eigenvalues, the use of an iterative procedure, as well as the task of guaranteed search for all modes whose frequencies belong to a given domain on the complex frequency plane.

In this paper, a modified spectral approach is proposed for calculating the complex frequencies of modes and the distributions of their fields in an open gyrotron resonator. This approach is a generalization of the methodology from [46] and is based on the linearization of RBC by spectral parameter. Due to the peculiarities of the geometry of the open gyrotron resonator, the developed approach makes it possible to calculate the complex frequency and field distribution of the main longitudinal type of oscillations with accuracy sufficient for practical applications by solving the linear matrix eigenvalue problem once without specifying an initial approximation. In addition, in most cases, one or two additional solutions to the linear matrix eigenvalue problem are required to calculate each subsequent higher type of oscillation.

The contents of the article are organized as follows. Section 1 presents the basic equations of the boundary value problem describing oscillations in an open gyrotron cavity. Here we also outline a technique for linearizing the boundary conditions of radiation, which makes it possible to reduce the solution of a nonlinear spectral problem to a sequence of solutions to linear spectral problems. Section 2 describes a method for reducing a boundary value problem in differential form to a linear generalized matrix eigenvalue problem (GMAEP) using the finite difference method. Section 3 provides a description of an iterative algorithm that allows one to calculate a given number of complex frequencies and field distributions of quasi-eigentypes of oscillations in an open resonator. The section 4 includes examples of calculations of longitudinal types of oscillations in open gyrotron resonators of various frequency ranges, the parameters of which are available from the literature. The Conclusion formulates the results obtained and the main

conclusions.

1. Basic equations and linearization of radiation boundary conditions

The geometry of the gyrotron resonator in the form of a weakly inhomogeneous hollow metal waveguide is shown in Fig. 1. It is assumed that the radius of the waveguide varies slowly along its axis. Neglecting the connection between waveguide modes with different radial indices, the boundary value problem describing the oscillations of the electromagnetic field in the resonator [40] consists of the inhomogeneous string equation

$$\frac{d^2F(z)}{dz^2} + h^2(\omega, z)F(z) = 0, \tag{1}$$

and radiation boundary conditions, which are set in planes perpendicular to the resonator axis and located in homogeneous parts of the waveguides to the left and right of the main volume of the resonator:

$$\begin{aligned} \left[\frac{dF(z)}{dz} - jh(\omega, z)F(z)\right]_{z=z_{\text{in}}} &= 0\,, \\ \left[\frac{dF(z)}{dz} + jh(\omega, z)F(z)\right]_{z=z_{\text{out}}} &= 0\,. \end{aligned} \tag{2}$$

In the equations (1)–(2) it is assumed that the field depends on time in the form $F(z) \sim \exp(j\omega t)$ and the following notation is introduced: $F(z)$ — dimensionless complex amplitude of the H_z component of the electromagnetic field in the resonator; $h(\omega, z)$ — local value of the longitudinal wavenumber of the TE_{mn}-mode; the value $h(\omega, z)$ depends on the coordinate z due to the change in the radius of the resonator $R(z)$ when displaced along its axis.

The boundary conditions (2) contain roots of the complex frequency function $h^2(\omega, z)$, so it is necessary to determine the rules for choosing branches of this function [40]:

$$\begin{aligned} &\text{Re}\,[h(\omega, z_{\text{in,out}})] > 0, \quad \text{если Re}\,\left[h^2(\omega, z_{\text{in,out}})\right] > 0\,, \\ &\text{Im}\,[h(\omega, z_{\text{in,out}})] < 0, \quad \text{если Re}\,\left[h^2(\omega, z_{\text{in,out}})\right] < 0\,. \end{aligned}$$

These conditions are based on the requirement: for any frequencies, solutions to the equation (1) in homogeneous sections of waveguides lying to the left and right of the region $z_{\text{in}} \leqslant z \leqslant z_{\text{out}}$ must represent waves that transfer energy in the direction from the central part of the resonator.

Taking into account the small ohmic losses in the resonator walls, we can write that $h^2(\omega, z) = h_r^2(\omega, z) - jh_i^2(\omega, z)$, where

$$\begin{aligned} h_r^2(\omega, z) &= \omega^2/c^2 - \nu_{mn}^2/R^2(z)\,, \\ h_i^2(\omega, z) &= (1-j)\delta_s \frac{\nu_{mn}^2}{R^3(z)} \left(1 + \frac{m^2}{\nu_{mn}^2 - m^2} \frac{\omega^2 R^2(z)}{c^2 \nu_{mn}^2}\right). \end{aligned} \tag{3}$$

In this formula, $h_r^2(\omega, z)$ is the square of the wave number of the operating mode TE_{mn} in the case of ideally conducting resonator walls, $-jh_i^2(\omega, z)$ — addition to the squared wave number due to the finite conductivity of the walls, $J'_m(x)$ — derivative of the Bessel function of order m, ν_{mn} — nth root of the equation $J'_m(\nu_{mn}) = 0$, c — speed of light, $\delta_s = \sqrt{2/(\mu_0 \omega \sigma)}$ — skin layer thickness, *sigma* — specific conductivity of the resonator wall material, μ_0 — magnetic

constant. The expression for $h_i^2(\omega, z)$ is derived by the method developed in [47]; it coincides with the formulas given in [48, 49].

Let us write $h_r^2(\omega, z)$ as follows:

$$h_r^2(\omega, z) = (\omega^2 - \omega_0^2)/c^2 + \nu_{mn}^2/R_0^2 \left[1 - R_0^2/R^2(z)\right],$$

where R_0 is the radius of the waveguide in some characteristic section, $\omega_0 = \nu_{mn}c/R_0$ is the critical frequency of the operating mode in this section. The value R_0 can be taken, for example, to be the radius of the homogeneous part of the resonator or the radius in the plane of transition from the interaction region to the expanding horn if there is no homogeneous part of the resonator.

Let L_0 be the characteristic size of the resonator, which can be taken as the length of a homogeneous part or its entire length. Assuming $\omega \approx \omega_0$, we introduce the dimensionless frequency parameter $\Omega = (\omega^2 - \omega_0^2)L_0^2/c^2 \approx 2(\nu_{mn}L_0/R_0)^2(\omega - \omega_0)/\omega_0$, dimensionless coordinate $\zeta = z/L_0$ and functions

$$\delta(\zeta) = (\nu_{mn}L_0/R_0)^2 \left(1 - \frac{R_0^2}{R^2(z)}\right),$$

$$d(\zeta) = (1 - j)(\nu_{mn}L_0/R_0)^2 \frac{\delta_s R_0^2}{R^3(\zeta)} \left(1 + \frac{m^2}{\nu_{mn}^2 - m^2} \frac{\omega^2 R^2(\zeta)}{c^2 \nu_{mn}^2}\right).$$

Note that $\delta(\zeta)$ does not depend on the frequency ω, and $d(\zeta)$ changes very little with frequency, since this change is determined mainly by the dependence of the skin layer thickness δ_s from frequency. In the expected range of frequencies of longitudinal modes, this dependence can be neglected. Therefore, in the formula for $d(\zeta)$ we can put $\omega = \omega_0$ and assume that this function also does not depend on frequency.

After all the redesignations, the equations (1)–(2) take the form

$$\frac{d^2F(\zeta)}{d\zeta^2} + [\Omega + \delta(\zeta) - jd(\zeta)]\, F(\zeta) = 0 \tag{4}$$

and

$$\begin{aligned} &\left[\frac{dF(\zeta)}{d\zeta} - j\sqrt{\Omega + \delta(\zeta) - jd(\zeta)}F(\zeta)\right]_{\zeta=\zeta_{\text{in}}} = 0, \\ &\left[\frac{dF(\zeta)}{d\zeta} + j\sqrt{\Omega + \delta(\zeta) - jd(\zeta)}F(\zeta)\right]_{\zeta=\zeta_{\text{out}}} = 0. \end{aligned} \tag{5}$$

The (4)–(5) equations are a boundary value problem of the type of the problem Sturm – Liouville eigenvalue, the solutions of which determine complex modes of oscillations in an open electrodynamic structure — a gyrotron resonator. The dimensionless frequency parameter Ω acts as a spectral parameter here. Note that the value Ω enters the boundary conditions (5) in a non-linear way, therefore, as noted in the Introduction, an iterative approach has to be used to solve it.

The method for solving the boundary value problem (4)–(5) is described below. Let us put in the equations (4)–(5) $\Omega = \Omega_0 + \tilde{\Omega}$, where Ω_0 is a given constant, and $\tilde{\Omega}$ is a small quantity in the sense that will be explained below. Then the square roots in the formulas (5) can be decomposed into a Taylor series by degrees of $\tilde{\Omega}$ and leave only the first two terms in the decomposition:

$$\sqrt{\Omega_0 + \tilde{\Omega} + \delta(\zeta_{\text{in,out}}) - jd(\zeta_{\text{in,out}})} \approx \sqrt{\Omega_0 + \delta(\zeta_{\text{in,out}}) - jd(\zeta_{\text{in,out}})} + \\ + \frac{\tilde{\Omega}}{2\sqrt{\Omega_0 + \delta(\zeta_{\text{in,out}}) - jd(\zeta_{\text{in,out}})}}. \tag{6}$$

Attenuation in the walls of the resonator is usually very small, so the condition $|\delta(\zeta_{\text{in,out}})| \gg |d(\zeta_{\text{in,out}})|$ is satisfied. Considering that the radii of the homogeneous parts of the waveguides in which the sections $\zeta_{\text{in,out}}$ are located differ significantly (by tens of percent or more) from the radius of the central part of the resonator, we can assume that $|\delta(\zeta_{\text{in,out}})| \sim (\nu_{mn} L_0/R_0)^2$.

For modern gyrotrons, the characteristic resonator dimensions R_0 and L_0, as well as the operating mode indices m and n are such that the relative frequency detuning from the critical one for longitudinal modes is $|\omega - \omega_0|/\omega_0 \leqslant 0.1$, and the parameter $(\nu_{mn} L_0/R_0)^2$ takes values from 10^2 to 10^4. Then, with a large margin, the inequality is true $|\delta(\zeta_{\text{in,out}})| \gg |\Omega|$. In this case, you can always choose the parameter Ω_0 so that the relation $|\delta(\zeta_{\text{in,out}}) + \Omega_0| \gg |\tilde{\Omega}|$. This is the condition for the parameter $\tilde{\Omega}$ to be small, under which terms of order $\tilde{\Omega}^2$ and higher can be ignored in the expansion (6). In particular, to calculate the first few longitudinal modes it is enough to put $\Omega_0 = 0$.

Let us introduce the notation $\kappa_{\text{in,out}} = \sqrt{\Omega_0 + \delta(\zeta_{\text{in,out}}) - jd(\zeta_{\text{in,out}})}$ and substitute the decomposition (6) in (4) and (5), as a result of which we obtain the differential equation of the boundary value problem in the form

$$\frac{d^2F(\zeta)}{d\zeta^2} + [\Omega_0 + \delta(\zeta) - jd(\zeta)]\, F(\zeta) = -\tilde{\Omega} F(\zeta)\,. \tag{7}$$

and RBC, linearized by the spectral parameter Ω, in the form

$$\begin{aligned} &\left.\frac{dF(\zeta)}{d\zeta}\right|_{\zeta=\zeta_{\text{in}}} - j\kappa_{\text{in}} F(\zeta_{\text{in}}) = \tilde{\Omega}\frac{j}{2\kappa_{\text{in}}} F(\zeta_{\text{in}})\,, \\ &\left.\frac{dF(\zeta)}{d\zeta}\right|_{\zeta=\zeta_{\text{out}}} + j\kappa_{\text{out}} F(\zeta_{\text{out}}) = -\tilde{\Omega}\frac{j}{2\kappa_{\text{out}}} F(\zeta_{\text{out}})\,. \end{aligned} \tag{8}$$

The new dimensionless frequency parameter $\tilde{\Omega}$ enters the equations (7), (8) linearly, therefore, when discretizing them, a linear GMAEP will be obtained, in which the spectral parameter is $\tilde{\Omega}$.

2. Discretization of boundary value problem equations

To obtain algebraic equations from the equations of a boundary value problem written in differential form, you can use finite element or finite difference methods. The first of them has the advantages that it can be applied to a non-uniform mesh, which can significantly reduce memory requirements, and also allows for simple generalization to the case of high-order finite elements, which improves the accuracy of the results obtained.

On the other hand, the finite difference method on a uniform grid in the case of one spatial coordinate is extremely simple to understand and implement in software. Therefore, a discretization method based specifically on the second approach will be described here.

Let us discretize the boundary value problem (7)–(8) by the finite difference method. To do this, we introduce a uniform grid on the segment $z_{\text{in}} \leqslant z \leqslant z_{\text{out}}$ with a step of Δz and a dimensionless step of $\Delta\zeta = \Delta z/L_0$. The number of grid nodes $N = (z_{\text{out}} - z_{\text{in}})/\Delta z + 1$, they are numbered as follows: $z_1 = z_{\text{in}}$, $z_i = z_1 + (i-1)\cdot\Delta z$, $i = 2, \ldots, N-1$, $z_N = z_{\text{out}}$. Replacing the second derivative in (7) by its symmetric discrete approximation in the inner nodes of the grid, we obtain the relations

$$\frac{1}{\Delta\zeta^2}\left(-F_{i-1} + 2F_i - F_{i+1}\right) - (\Omega_0 + \delta_i - jd_i)\, F_i = \tilde{\Omega} F_i, \quad i = 2, \ldots, N-1. \tag{9}$$

In the first and last nodes, the boundary conditions (8) must be additionally taken into account. For the first node, we have an equation similar to (9), c$i = 1$, as well as the finite difference form

of the first of the boundary conditions (8)

$$\frac{1}{\Delta\zeta^2}\left(-F_2+2F_1-F_0\right)-\kappa_{\text{in}}^2F_1=\tilde{\Omega}F_1,$$
$$\frac{1}{2\Delta\zeta}\left(F_2-F_0\right)-j\left(\kappa_{\text{in}}+\tilde{\Omega}/(2\kappa_{\text{in}})\right)F_1=0\,.$$

Excluding from these formulas the field F_0 in the dummy node with the number 0, we obtain the equation

$$\left(\frac{1}{\Delta\zeta^2}+\frac{\kappa_{\text{in}}^2}{2}+j\frac{\kappa_{\text{in}}}{\Delta\zeta}\right)F_1-\frac{1}{\Delta\zeta^2}F_2=\tilde{\Omega}\left(\frac{1}{2}-\frac{j}{2\kappa_{\text{in}}\Delta\zeta}\right)F_1. \tag{10}$$

Similarly, the difference equation for the last node with the number is presented N:

$$-\frac{1}{\Delta\zeta^2}F_{N-1}+\left(\frac{1}{\Delta\zeta^2}+\frac{\kappa_{\text{out}}^2}{2}+j\frac{\kappa_{\text{out}}}{\Delta\zeta}\right)F_N=\tilde{\Omega}\left(\frac{1}{2}-\frac{j}{2\kappa_{\text{out}}\Delta\zeta}\right)F_N\,. \tag{11}$$

By collecting the formulas (9)–(11) in the correct order, we obtain a system of linear algebraic equations with respect to the values of the field at the nodes of the grid, which is written in matrix form as

$$[\hat{A}(\Omega_0)]\{F\}=\tilde{\Omega}[\hat{B}(\Omega_0)]\{F\}. \tag{12}$$

Here $[\hat{A}(\Omega_0)]$ — a tridiagonal symmetric complex matrix of the order $N\times N$, $[\hat{B}(\Omega_0)]$ — a diagonal complex matrix of the order $N\times N$, $\{F\}=[F_1,F_2,\ldots,F_N]^T$ — column vector of length N, symbol T — sign of the transpose operation. Expressions for matrix elements $[\hat{A}]$ and $[\hat{B}]$[1] are easily obtained from formulas (9)–(11).

3. The method of calculating eigenvalues with iterative refinement of the boundary conditions of radiation

The equation (12) is an GMAEP for a pair of matrices $([\hat{A}],[\hat{B}])$ [50–52], and $\tilde{\Omega}$ is an eigenvalue (eigenvalue) for this problem. Note that the elements of the matrices $[\hat{A}]$ and $[\hat{B}]$ do not depend on $\tilde{\Omega}$, therefore this spectral problem is linear and standard methods of computational linear algebra can be used to solve it. In particular, to run the algorithm for searching for eigenvalues and eigenvectors of this problem, no special selection of any initial approximations is required. In most programs used for the numerical solution of linear GMAEP, the initial ones are not approximations for the ES, but approximations for eigenvectors, the components of which are randomly selected.

The order of the matrix problem (12) in the case of a large N can reach several thousand, respectively, it has the same number of ES, but of them only a small number of the smallest modulo ES corresponding to the lowest longitudinal modes are of practical interest. When calculating complex types of vibrations in a gyrotron resonator, their number most often does not exceed ten or, in rare cases, twenty. In this case, the solution of the (12) problem can be effectively carried out by the Arnoldi [51, 52] method implemented in the ARPACK [53] library. The procedures for solving linear GMAEP included in this library allow you to calculate the required number of eigenvalues lying in a given part of the spectrum, for example, those closest to zero on the complex plane or having the smallest positive values of the real part, etc. Using this

[1]Next, for brevity, we will omit the notation of the dependencies of these matrices on Ω_0.

property, as well as the procedure for reverse shifting eigenvalues, allows you to build an iterative algorithm for calculating a given the number of eigenvalues of a nonlinear problem (4)–(5).

The procedure for the reverse shift of the ES for the equation (12) is as follows. Let's put $\tilde{\Omega} = \Omega_s + 1/\lambda$ in it, move the term proportional to Ω_s to the left side and multiply the resulting equation on the left by $([\hat{A}] - \Omega_s[\hat{B}])^{-1}$. As a result, instead of (12) we get

$$\left([\hat{A}] - \Omega_s[\hat{B}]\right)^{-1} [\hat{B}]\{F\} = \lambda\{F\}, \tag{13}$$

where $\lambda = 1/(\tilde{\Omega} - \Omega_s)$. The ratio (13) is no longer a generalized, but a standard eigenvalue problem for the matrix $([\hat{A}] - \Omega_s[\hat{B}])^{-1}[\hat{B}]$, which stands on the left side of this equation. If λ_i, $i = 1, 2, \ldots, n$ — the eigenvalues of the problem (13) having the largest positive real parts and arranged in decreasing order, then $\tilde{\Omega}_i = \Omega_s + 1/\lambda_i$, $i = 1, 2, \ldots, n$ will be n eigenvalues of GMAEP(12) satisfying the condition $\operatorname{Re}\tilde{\Omega}_i > \operatorname{Re}\Omega_s$ and ordered as the values increase $\operatorname{Re}\tilde{\Omega}_i$.

Note that in the algorithm implemented in the ARPACK package to solve the standard matrix problem in the form of (13), it is not required to explicitly calculate the matrix on the left in this equation. Instead, it is enough to have two procedures, one of which calculates the result of multiplying an arbitrary vector of length N by the matrix $[\hat{B}]$, and the second returns the vector $\{X\}$ — the result of solving the linear equation $([\hat{A}] - \Omega_s[\hat{B}])\{X\} = \{Y\}$ for an arbitrary vector $\{Y\}$ of length N.

Thus, by choosing the value of the shift Ω_s, you can calculate the required number of eigenvalues of GMAEP(12) in the desired part of the spectrum. Note that the choice of Ω_s does not affect the values of the resulting ES, but only determines which ES for a pair of matrices $([\hat{A}], [\hat{B}])$ will be calculated.

In practice, when modeling vibrations in a gyrotron resonator, depending on specific applications, two problem statements arise. In the first case, this is the calculation of the complex frequency and the corresponding field distribution in the resonator only for the main longitudinal mode of oscillations. Knowledge of these parameters allows, using the formulas of the linear theory of the gyrotron in the approximation of the fixed structure of the field [2, 54–56], to quickly calculate the position of the oscillation zone for the main mode on the plane of the parameters B_0, I_{st} (here B_0 — magnetic field, I_{st} — the starting current of the soft occurrence of vibrations), as well as the minimum value of the starting current. In the second case, it is necessary to accurately calculate the complex frequencies and field distributions for several lower longitudinal modes. Such a need arises, for example, when developing gyrotrons with frequency tuning due to changes in the magnetic field (see, for example, [6–8]).

For each of these cases, two different algorithms can be used to solve GMAEP with RBC linearization by spectral parameter. In the first variant, it is enough to simply put the parameter $\Omega_0 = 0$ in the equation (12) and find one eigenvalue of this problem with the smallest real part. As the tests conducted for a large number of resonators show, the oscillation parameters calculated with great accuracy (on the order of 6-8 significant digits for frequency and 4-6 significant digits for Q-factor) coincide with the results of solving the boundary value problem by other methods, in particular, the targeting method. Examples of such calculations are given in the next section.

In the second variant, to find several longitudinal modes, you can use an iterative procedure that allows you to sequentially calculate a given number of ES, starting with the main mode. In this case, the complex frequency of the first mode is found using the algorithm from the previous paragraph, and the initial approximations for the complex frequencies of the mode with the number $i > 1$ will be calculated automatically during the iterations performed when calculating the mode with the number $i - 1$.

The pseudocode of the algorithm for searching for multiple eigenvalues is shown in Fig. 2

```
function OmegaResult = GyrCavIteration[n, Omega0, tol, alpha]
% Input parameter:
%
% Omega0 - lower bound for searching eigenvalues;
% n - number of eigenvalues;
% tol - convergence criterion;
% alpha - parameter for settings the shift for the matrix
%         eigenvalue problem, 0 < alpha < 1;
%
% Result:
%    Complex eigenvalues in array OmegaResult(i), i=1,...n

%  initial settings

   OmegaNew = Omega0;
   i = 0;
% cycle for eigenvalues searching
   while i<= n

% cycle for iterative clarification of the eigenvalue
      while true
% Calculation of matrices A and B for a given value OmegaNew
        ..........................................
        OmegaShift = OmegaNew - (1-alpha)*real(OmegaNew);
% Solving the generalized matrix eigenvalue problem (13)
% and finding two eigenvalues lambda(k), k = 1,2 with
% the largest real(lambda), such that real(lambda(1)) >
% real(lambda(2);
        ..........................................
        OmegaPrev = OmegaNew;
        OmegaNew  = OmegaNew + OmegaShift + 1/lambda(1);
        OmegaNext = OmegaNew + OmegaShift + 1/lambda(2);

% convergence test
        if abs(OmegaNew-OmegaPrev) < tol*max(abs(OmegaNew), ...
                                             abs(OmegaPrev))
           break;
        end
%
      end    %   end internal while
% convergence achieved
      OmegaResult(i) = OmegaNew;
% initial value for the next eigenvalue
      OmegaNew = OmegaNext;
      i = i + 1;
   end    % end external while
end       % end module
```

Fig 2. Pseudocode of the function for eigenvalues searching by iterative clarification of the linearized radiation boundary conditions. The dot lines must contain code that implements the operations described in the previous comment

and consists of the following. Let the eigenvalues of the matrix problem (12) be arranged in ascending order of their real parts, $i-1$ of the first ES is found, and there is an initial approximation Ω_{i0} for the ES with the number i. If we form the matrices $[\hat{A}(\Omega_{i0})]$ and $[\hat{B}(\Omega_{i0})]$ and shift Ω_s set so that the condition $\mathrm{Re}\,(\Omega_{i-1}) < \mathrm{Re}\,(\Omega_s) < \mathrm{Re}\,(\Omega_{i0})$ is satisfied, then using the reverse shift procedure to solve the matrix problem as the first calculated NW will give an improved approximation for the ith NW. When repeating this process, the value of Ω_{i0} converges to the desired eigenvalue of Ω_i, while at each iteration the value of $|\Omega_{i0} - \Omega_i|$ becomes smaller and smaller, rapidly tending to zero. Therefore, the solution for the mode with the number i of the linear GMAEP(12) obtained by discretizing the boundary value problem with linearized radiation boundary conditions(7)–(8) tends to solve a nonlinear spectral boundary value problem (4)–(5).

It remains to determine how, after calculating the ES with the number i, to set the initial approximation for searching for the next ES. Here it can be taken into account that when solving GMAEP using the Arnoldi method, even if only one ES is calculated, several of them are always calculated, therefore, at each iteration of the process described in the previous paragraph, except for the exact value of the i-th eigenvalue[2], Naturally, a good enough approximation is found to run iterations of the search for the next ES.

Note that in the considered procedure, at each iteration of the internal cycle of the algorithm (see Fig. 2) a new, more appropriate value is calculated for the value Ω_0, near which RBC linearization occurs when deriving the equations (7)–(8). At the same time, linearized RBC models radiation processes more and more precisely for the mode that is calculated at this step of the external cycle of the eigenmode spectrum search procedure. Therefore, the proposed approach can be called a method for calculating resonator modes with iterative refinement of the radiation boundary conditions.

The vast majority of the time spent solving GMAEP in the ARPACK code is spent calculating eigenvalues; it takes much less time to calculate eigenvectors, therefore, each time the procedure is called from the ARPACK library, the need for simultaneous calculation of both eigenvalues and eigenvectors of the problem is established. As a result, at the output of the entire iterative process, we get a given number of ES and eigenvectors. The components of the latter are the values of the complex amplitude of the field of the calculated modes at the nodes of the grid.

Practical calculations show that for the internal convergence of the solution for the main mode, 3 iterations of the internal cycle of the algorithm are required (see Fig. 2), and for each subsequent mode there are 2 iterations, while in each case the last iteration is needed to check convergence. In general, to calculate n eigenmodes, it is necessary to solve the GMAEP approximately $2n+1$ times. For $n < 10$, this value is disproportionately less than the required number of solutions to the Cauchy problem for the differential equation (1) in the targeting method.

A Certificate of state registration of the computer program [57] was obtained for the program in which this technique is implemented. The program is written in the programming languages Wolfram Mathematica (interface) and Fortran (calculation module) and runs on Windows 10 or Windows 11 OC. Without any changes, the program can be recompiled for Linux OS.

[2]The term «exact value of the ES» is used here in the sense that it is the value of the ES of a nonlinear boundary value problem, found taking into account the error of its discretization, the convergence criterion of the iterative procedure and the convergence criterion of the Arnoldi method in the ARPACK library.

4. Test examples of resonators calculation

This section contains the results of test calculations of resonators of several gyrotrons operating in various ranges — from the long-wavelength part of the millimeter to the submillimeter wavelength range. For the convenience of references, the resonators for various test cases are indicated by a number in the Table 1 and the following data are given for each of them: range, type of operating mode, conductivity of the cavity walls used in calculations, reference to the source. In these links you can find complete data on the geometry of the resonators and other necessary parameters. For all examples, the results of modeling the main or several longitudinal modes in other ways are also given, which allows us to draw conclusions about the accuracy of the proposed method.

Schematic images of the resonators modeled in the tests, as well as the values or designations of their geometric dimensions are shown in Fig. 3. For resonators from tests 2–5, the dimensions are shown in Table 2.

Table 1. Gyrotron cavities for test calculations

Test number	Frequency, GHz	Operating mode	Wall conductivity, S/m	Link to the source
1	391	TE_{85}	$3{\cdot}10^7$	[58]
2	140	TE_{03}	∞	[37]
3	42	TE_{03}	∞	[37]
4	140	$TE_{10,4}$	∞	[37]
5	170	$TE_{34,10}$	$3{\cdot}10^7$	[59]

Table 2. Geometry parameters of the cavities 2–5 with profile shown in fig. 1, *b*

Parameter	Operating frequency, operating mode			
	140 GHz, TE_{03}	42 GHz, TE_{03}	42 GHz, $TE_{10,4}$	170 GHz, $TE_{34,10}$
L_1, mm	18.9	30.0	10.0	8
L_2, mm	10.0	44.0	11.0	13
L_3, mm	10.1	46.0	12.0	16
θ_1, °	0.5	2.0	5.0	2.8
θ_2, °	3.0	3.0	3.0	3.5
R_0, mm	3.47	11.57	8.11	20.95

4.1. Modeling of the main oscillation modes in resonators from tests 1-5. First, let's consider the results of calculations of the main types of vibrations for each resonator presented in Table 1. In this subsection, the calculation of the main mode was carried out using a simplified method, when a single ES of the linear GMAEP (12) with the smallest value $\mathrm{Re}\,(\tilde{\Omega})$, while $\Omega_0 = 0.0$ was assumed. Thus, for each of the 1–5 resonators, the matrix problem was solved only once. The values of frequencies and Q-values of the main modes calculated in this way are shown in Table 3. For comparison, in the same table, the last two columns show the corresponding values calculated by the targeting method using the [34] program. It can be seen that for all resonators, the frequency values calculated in two ways differ by no more than 2 units in the eighth sign, and the Q-values — by no more than 3 units in the fourth sign. These results confirm the remark from the section 3 that in the case of calculating only the main mode, it is sufficient to use a simplified technique, while the results obtained for the mode parameters

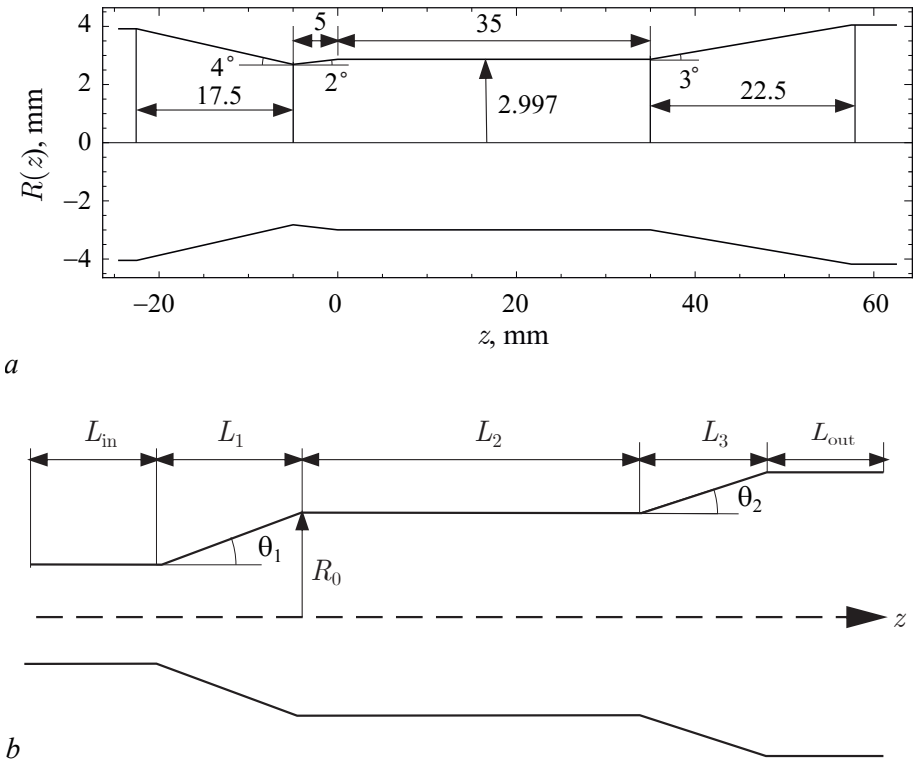

Fig 3. Cavities profiles considered in the tests: *a* — cavity for continuous frequency tunable gyrotron for spectroscopy studies [58]; *b* — profile of the cavities for tests from [37, 59]. All dimensions on the figure 3, *a* are given in mm

demonstrate very high accuracy.

The distributions of the fields of the main modes calculated in this way in all cases coincide graphically with the images of the fields obtained by solving a nonlinear spectral problem using an iterative technique. For some resonators, examples of these distributions will be given below.

Table 3. Frequencies and quality factors of the fundamental modes for the gyrotron cavities from tests 1–5

Resonator number	Spectral approach with RBC linearization		Method of targeting	
	Frequency, GHz	Diffraction Q-factor	Frequency, GHz	Diffraction Q-factor
1	391.47013	16631.3	391.47013	16630.8
2	140.22593	849.3	140.22592	849.0
3	42.03745	1115.2	42.03745	1115.2
4	140.12867	585.5	140.12869	585.7
5	170.00732	1394.2	170.00731	1394.09

4.2. A gyrotron on the TE_{85} mode with an operating frequency of 391 GHz. As a further example, the gyrotron resonator from [58] is considered, which operates on a second cyclotron harmonic with an operating frequency of 391 GHz and with continuous frequency

tuning in the range of about 2 GHz. The working mode of the gyrotron is $TE_{8.5}$. The device is intended for use in spectroscopic nuclear magnetic resonance installations using the effect of dynamic polarization of nuclei. The necessary frequency tuning is provided by the interaction of the electron beam with the fields of the oncoming components of the TE_{85q} modes when the magnetic field changes. Here, the longitudinal fashion index q varies in the range $q = 1...6$. The dependence of the resonator radius on the longitudinal coordinate, shown in Fig. 3, *a*, taken from [58]. The radius and length of the homogeneous part of the resonator are $R_0 = 2.997$ mm and $L_0 = 35$ mm. The calculated conductivity of the cavity walls is $\sigma = 3 \times 10^7$ Cm/m.

Note that in order to ensure frequency tuning due to the interaction of the beam with various longitudinal types of oscillations, high-order modes must have a relatively high Q factor in order to reduce the inrush current for them. Therefore, the resonator in Fig. 3, *a* has a large ratio of $L_0/R_0 \approx 11.7$ and a relatively large opening angle of the expanding horn at the right end of the resonator. This provides significant reflections of the wave in the waveguide from the transition of the homogeneous part of the resonator into the expanding horn.

The values of frequencies and Q-values of longitudinal modes calculated for this resonator for $q = 1...6$ are shown in the Table 4. The second and third columns of the table show the frequencies and Q-values obtained using the method developed in this article; the last two columns contain the same values calculated by the targeting method using the same program as in the previous example. The frequencies calculated by the two methods differ by no more than 2 units in the 8th significant digit, and the Q-factor - by 1-2 units in the fourth significant digit. Taking into account the different numerical approaches used in these techniques, it can be assumed that the results obtained with their help are practically the same.

In Fig. 4 shows the field distributions of complex modes in this resonator. The modules of complex field amplitudes are displayed in solid black lines, and their arguments are shown in orange lines. The dotted line corresponds to the resonator profile in arbitrary units. The fields calculated by both methods (spectral approach and targeting method) for all modes coincide with graphical accuracy.

4.3. Gyrotron resonators with frequencies of 42 GHz and 140 Hz [37]. The work [37] describes a set of GYROCOMPASS programs for computer simulation of gyrotron operation in different modes, including for calculating the parameters of a hollow resonator without a beam. The three gyrotrons shown in Table 1 are taken as test examples numbered 2–4. Calculations of these resonators were carried out and the results were compared with the data from the article [37]. The results of the comparison are summarized in the Table 5. It contains the values of frequencies and Q-values of the main longitudinal mode for three resonators,

Table 4. Frequencies and quality factors of the axial modes of the gyrotron cavity with operating mode TE_{85} [58]

q	Spectral approach with RBC linearization		Method of targeting	
	Frequency, GHz	Quality factor	Frequency, GHz	Quality factor
1	391.47013	16631.3	391.47013	16630.8
2	391.53397	13143.0	391.53397	13141.6
3	391.64034	9742.4	391.64034	9740.3
4	391.78919	7156.4	391.78919	7154.2
5	391.98044	5340.3	391.98045	5338.5
6	392.21399	4080.6	392.21401	4079.5

obtained in two ways: using the COAXIAL code developed earlier by O. Dumbrice, and using the GYROCOMPU code, as well as the values of the same values calculated using the methodology developed in this article.

Table 5. Comparison of frequencies and diffraction quality factors of the fundamental axial modes of the cavities with data from [37]

Тип колебаний	GYROCOMPU		COAXIAL		Spectral approach with RBC linearization	
	Frequency, GHz	Diffraction Q-factor	Frequency, GHz	Diffraction Q-factor	Frequency, GHz	Diffraction Q-factor
TE_{031}	140.223	857.1	140.226	849.0	140.226	849.3
TE_{031}	42.037	1136.6	42.037	1115.0	42.037	1115.2
$TE_{10,4,1}$	140.129	588.0	140.129	586.0	140.129	585.7

As follows from the Table 5, the frequency values of the main modes obtained using all three codes are practically the same. The diffraction Q-values calculated using the COAXIAL code and the proposed method also coincide, and the GYROCOMPU program gives values for Q-values

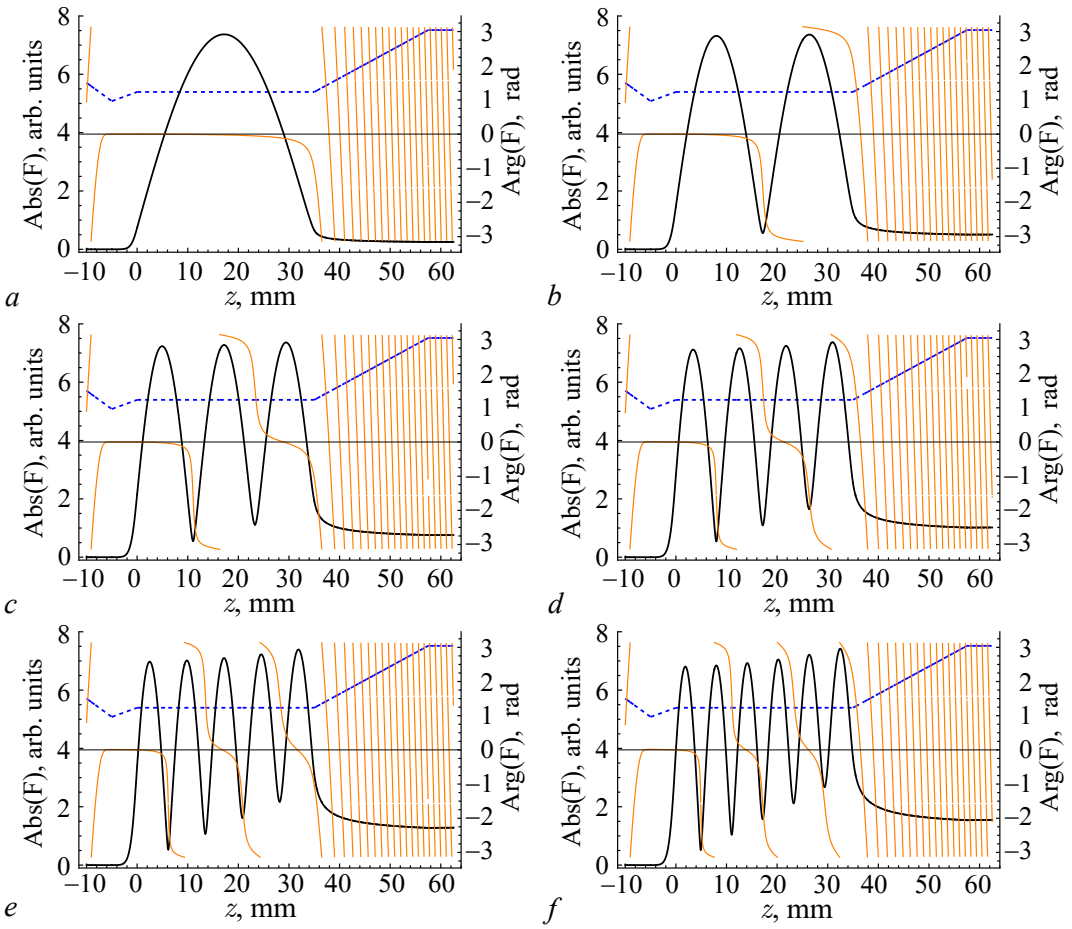

Fig 4. Field distributions of the first six hight order axial modes of a gyrotron cavity with an operating mode of TE_{85} and a frequency 391 GHz. Fig. *a–f* correspond to modes with axial indices $q = 1...6$. Solid black lines are the modules of the complex amplitude of the field in arbitrary units, orange lines — phases of the complex amplitude, blue dotted line — cavities profile (color online)

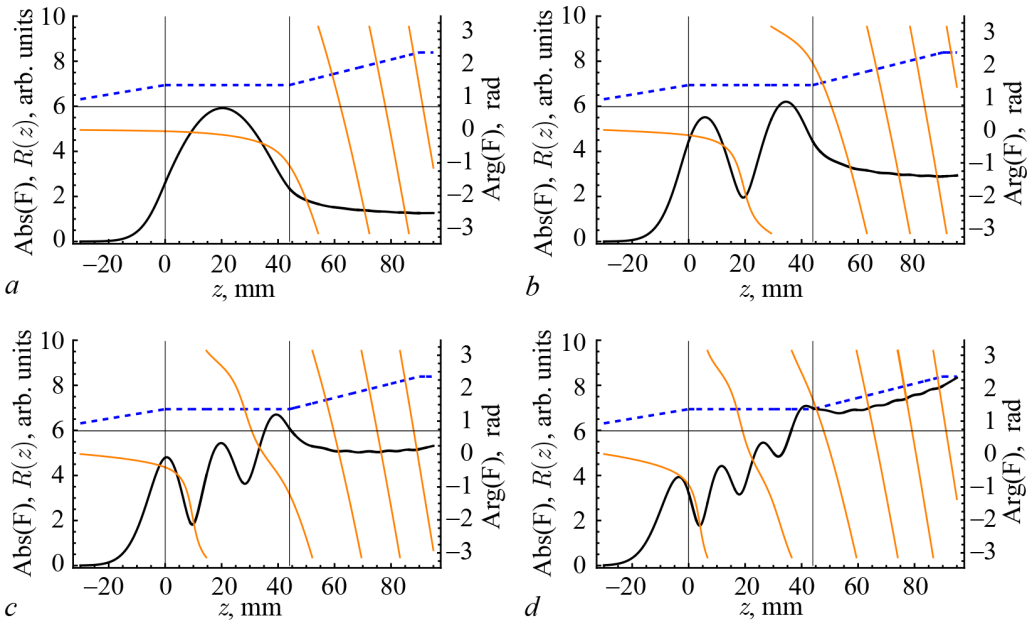

Fig 5. Fields distributions of four cavity axial modes for gyrotron with operating mode TE_{03q} and frequency 42 GHz. Figures *a*–*d* correspond to modes with axial indexes $q = 1...4$. Solid curves — modules of the complex field amplitude (arbitrary units), orange curves — phases of the complex field amplitude, blue dashed line — cavities profile (color online)

exceeding the results of the other two programs by 5-10%. In the article [37], this difference is explained by the difference in numerical techniques used in the COAXIAL and GYROCOMPU programs, and not by a defect in any of them.

Using a spectral approach with iterative refinement of the RBC, calculations of frequencies, Q-values and spatial distributions for higher longitudinal modes in resonators from tests 2-4 were also performed, and the results obtained were compared with the results of the targeting method [34]. For all resonators and for all calculated longitudinal modes, the same complete agreement of these results with each other is observed as for the resonator from test 1. For example, in Fig. 5 shows the field patterns of the first four modes in the resonator from test 3. The colors and outlines of the various curves in this figure are similar to the curve parameters taken in Fig. 4.

4.4. Test case 5. Gyrotron resonator for plasma heating [59]. The gyrotron described in [59] is designed as a prototype gyrotron for plasma heating. According to the projected output parameters stated in this article, it should generate power in excess of 1 MW at a frequency of 170 GHz with an electronic efficiency exceeding 35The voltage and current are 78...82 kV and 40 A, respectively. The working mode of the resonator$TE_{34,10,1}$.

The extreme parameters of this gyrotron require careful design of the resonator. High thermal loads lead to the need to maximize the reduction of the diffraction Q-factor of the working mode of vibrations while maintaining a high value of the ohmic Q-factor. The effective length of the working mode, defined in [60] by the formula

$$L_{\text{eff}} = \frac{\pi}{\sqrt{(2\pi f/c)^2 - (\nu_{mn}/R_0)^2}},$$

at the generation frequency of f =170 GHz is $L_{\text{eff}} \approx 18.8$mm, with the ratio $L_{\text{eff}}/R_0 \approx 0.9$ is extremely small. The high azimuthal and radial indices of the working mode and the large

radius of the resonator determine the high value of the ohmic quality factor, which, if evaluated according to the well-known formula [2], is$Q_{\text{ohm}} \approx 74420$.

With such resonator parameters, the complex frequency of the main mode $TE_{34,10,1}$ appears on the complex plane significantly separated from the frequencies of modes with higher longitudinal indices. This has a beneficial effect on increasing the starting currents for these modes and, consequently, on the stability of oscillations in the main mode.

If the targeting method is used to calculate the oscillation spectrum, this separation of complex frequencies leads to difficulty in finding initial approximations for each of these modes. At the same time, as calculations show, the modified spectral approach proposed here easily copes with this task and calculates the required number of complex frequencies one by one using the iterative algorithm described in the section3.

In the Table 6 the results of calculations of the frequencies and Q-values of the oscillations of the first four longitudinal modes of the resonator in question are presented. The coincidence of the results for the two lower modes obtained by the proposed method and the run-through method can be considered good, but as the mode number increases, this coincidence worsens. It can be assumed that this deterioration is due to the fact that this resonator has a significant narrowing of the waveguide at the cannon end of the resonator and at this point the wave in the waveguide becomes highly supercritical. Under these conditions, the equation (4) acquires the properties of a rigid differential equation [61], as a result of which the accuracy of solving the Cauchy problem in the run-through method decreases. However, this assumption needs additional verification. The distributions of the fields of the calculated modes look similar to the fields in Fig. 5 and are not listed here.

Table 6. Frequencies and diffraction quality factors of HOAM for gyrotron cavity with operating frequency 170 GHz [59]

q	Spectral approach with RBC linearization		Method of targeting	
	Frequency, GHz	Diffraction Q-factor	Frequency, GHz	Diffraction Q-factor
1	170.00732	1393.5	170.00731	1394.1
2	170.56715	356.5	170.56692	356.0
3	171.46104	210.9	170.46182	211.6
4	172.41215	154.3	172.40427	152.8

Conclusion

The article describes a spectral approach with iterative refinement of the radiation boundary conditions for solving a boundary value problem describing quasi-spatial oscillations in an open gyrotron resonator. The method allows us to calculate the spectrum of longitudinal quasi-spatial modes, which implies the calculation of their frequencies, Q-values (diffraction, ohmic and total), as well as distributions of complex amplitudes of the mode fields.

The main feature of the method is that when using it, there is no need to specify initial approximations to search for complex mode frequencies, which is the main problem when using other iterative methods to solve this problem, for example, the targeting method. Moreover, if it is necessary to calculate the parameters of only the main oscillation mode of an open resonator, then this technique allows us to obtain them after a single solution of the generalized matrix eigenvalue problem, without additional iterations.

The developed technique can be generalized to the case of equations of the linear theory of the gyrotron and used to develop new methods for analyzing conditions of soft self-excitation in gyrotron generators.

References

1. Flyagin VA, Gaponov AV, Petelin MI, Yulpatov VK. The gyrotron. IEEE Transactions on microwave theory and techniques. 1977;25(6):514–521. DOI: 10.1109/TMTT.1977.1129149.
2. Nusinovich GS. Introduction to the Physics of Gyrotron. Baltinore and London: Johns Hopkins University Press; 2004. 335 p.
3. Kartikeyan MV, Borie E, Thumm M. Gyrotrons: High-Power Microwave and Millimeter Wave Technology. Berlin, Heidelberg, New York: Springer Verlag; 2003. 228 p.
4. Thumm M. Progress on gyrotrons for ITER and future thermonuclear fusion reactors. IEEE transactions on plasma science. 2011;39(4):971–979. DOI: 10.1109/TPS.2010.2095042.
5. Glyavin MY, Idehara T, Sabchevski SP. Development of THz gyrotrons at IAP RAS and FIR UF and their applications in physical research and high-power THz technologies. IEEE Transactions on Terahertz Science and Technology. 2015;5(5):788–797. DOI: 10.1109/TTHZ.2015.2442836.
6. Hornstein MK, Bajaj VS, Griffin RG, Kreischer KE, Mastovsky I, Sirigiri JR, Shapiro MA, Temkin RJ. Second harmonic operation at 460 GHz and broadband continuous frequency tuning of a gyrotron oscillator. IEEE Transactions on Electron Devices. 2005;52(5):798–807. DOI: 10.1109/TED.2005.845818.
7. Chang TH, Idehara T, Ogawa I, Agusu L, Kobayashi S. Frequency tunable gyrotron using backward-wave components. Journal of Applied Physics. 2009;105(6):063304. DOI: 10.1063/1.3097334.
8. Torrezan AC, Han ST, Mastovsky I, Shapiro MA, Sirigiri JR, Temkin RJ, Barnes AB, Griffin RG. Continuous-wave operation of a frequency-tunable 460-GHz second-harmonic gyrotron for enhanced nuclear magnetic resonance. IEEE Transactions on Plasma Science. 2010;8(6): 1150–1159. DOI: 10.1109/TPS.2010.2046617.
9. Torrezan AC, Shapiro AC, Sirigiri JR, Temkin RJ, Griffin RG. Operation of a continuously frequency-tunable second-harmonic CW 330-GHz gyrotron for dynamic nuclear polarization. IEEE Transaction on Electron Devices. 2011;58(8):2777–2783. DOI: 10.1109/TED.2011.2148721.
10. Glyavin MYu, Denisov GG, Zapevalov VE, Koshelev MA, Tretyakov MYu,Tsvetkov AI. High power terahertz sources for spectroscopy and material diagnostics. Physics-Uspekhi. 2016; 59(6):595–677. DOI: 10.3367/ufne.2016.02.037801.
11. Sabchevski S, Glyavin M. Development and application of THz gyrotrons for advanced spectroscopic methods. Photonics. 2023;12(2):189–207. DOI: 10.3390/photonics10020189.
12. Siegel PH. Terahertz technology in biology and medicine. IEEE Transactions on Microwave Theory and Techniques. 2004;52(10):2438–2447. DOI: 10.1109/TMTT.2004.835916.
13. Pilossof M, Einat M. Note: A 95 GHz mid-power gyrotron for medical applications measurements. Review of Scientific Instruments. 2015;86(1):016113. DOI: 10.1063/1.4906507.
14. Cheon H, Yang HJ, Lee SH, Kim YA, Son JH. Terahertz molecular resonance of cancer DNA // Scientific Reports. 2016;6(1):37103. DOI: 10.1038/srep37103.
15. Miyoshi N, Idehara T, Khutoryan E, Fukunaga Y, Bibin AB, Ito S, Sabchevski SP. Combined hyperthermia and photodynamic therapy using a sub-THz gyrotron as a radiation source. Journal of Infrared, Millimeter, and Terahertz Waves. 2016;37(8):805–814. DOI: 10.1007/s10762-016-0271-z.
16. Bykov Y, Eremeev A, Glyavin M, Kholoptsev V, Luchinin A, Plotnikov G, Denisov A,

Bogdashev G, Kalynova V, Semenov N, Zharova N. 24-84-GHz gyrotron systems for technological microwave applications. IEEE Transactions on Plasma Science. 2004;32(1):67–72. DOI: 10.1109/TPS.2004. 823904.
17. Bratman VL, Bogdashov AA, Denisov GG, Glyavin MYu, Kalynov YuK, Luchinin AG, Manuilov VN, Zapevalov VE, Zavolsky NA, Zorin VG. Gyrotron development for high power THz technologies at IAP RAS. Journal of Infrared, Millimeter, and Terahertz Waves. 2012;33(7): 715–723. DOI: 10.1007/s10762-012-9898-6.
18. Aripin H, Mitsudo S, Prima ES, Sudiana IN, Tani S, Sako K, Fujii Y, Saito T, Idehara T, Sano S, Purwasasmita BS, Sabchevski S. Structural and microwave properties of silica xerogel glass-ceramic sintered by sub-millimeter wave heating using a gyrotron. Journal of Infrared, Millimeter, and Terahertz Waves. 2012;33(12):1149–1162. DOI: 10.1007/s10762-012-9925-7.
19. Glyavin M, Sabchevski S, Idehara T, Mitsudo S. Gyrotron-based technological systems for material processing – current status and prospects. Journal of Infrared, Millimeter, and Terahertz Waves. 2020;41(8):1022–1037. DOI: 10.1007/s10762-020-00727-w.
20. Federici J, Moeller L. Review of terahertz and subterahertz wireless communications. Journal of Applied Physics. 2010;107(11):111101. DOI: 10.1063/1.3386413.
21. Idehara T, Mitsudo S, Ogawa I. Development of high-frequency, highly stable gyrotrons as millimeter to submillimeter wave radiation sources. IEEE Transactions on Plasma Science. 2004;32(3):910–916. DOI: 10.1109/TPS.2004.827599.
22. Idehara T, Tsuchiya H, Watanabe O, Agusu L, Mitsudo S. The first experiment of a THz gyrotron with a pulse magnet. International Journal of Infrared and Millimeter Waves. 2006;27(3):319–331. DOI: 10.1007/S10762-006-9084-9.
23. Glyavin MYu, Luchinin AG, Golubiatnikov GYu. Generation of 1.5-kW, 1-THz Coherent Radiation from a Gyrotron with a Pulsed Magnetic Field. Phys. Rev. Lett. 2008;100:015101. DOI: 10.1103/PhysRevLett.100.015101.
24. Bratman VL, Kalynov YuK, Manuilov VN. Large-orbit gyrotron operation in the terahertz frequency range. Phys. Rev. Lett. 2009;102:245101. DOI: 10.1103/PhysRevLett.102.245101.
25. Bandurkin I, Fedotov A, Glyavin M, Idehara T, Malkin A, Manuilov V, Sergeev A, Tsvetkov A, Zaslavsky V, Zotova I. Development of third-harmonic 1.2-THz gyrotron with intentionally increased velocity spread of electrons. IEEE Transactions on Electron Devices. 2020;67(10):4432–4436. DOI: 10.1109/TED.2020.3012524.
26. Botton M, Antonsen TM, Levush B, Nguyen KT, Vlasov AN. MAGY: A time-dependent code for simulation of slow and fast microwave sources. IEEE Transactions on Plasma Science. 1998;26(3):882–892. DOI: 10.1109/27.700860.
27. Stock A, Neudorfer J, Riedlinger M, Pirrung G, Gassner G, Schneider R, Roller S, Munz CD. Three-dimensional numerical simulation of a 30-GHz gyrotron resonator with an explicit high-order discontinuous-Galerkin-based parallel article-in-cell method. IEEE Transactions on Plasma Science. 2012;40(7):1860–1870. DOI: 10.1109/TPS.2012.2195509.
28. Lin MC, Smithe DN, Guss WC, Temkin RJ. Hot test of gyrotron cavity interaction using a 3D CFDTD PIC method. 15th IEEE International Vacuum Electronics Conference. 2014. P. 87–88. IEEE. DOI: 10.1109/IVEC.2014.6857503.
29. Rozental RM, Tai EM, Tarakanov VP, Fokin AP. Using the 2.5-dimensional PIC code for simulating gyrotrons with nonsymmetric operating modes. Radiophysics and Quantum Electronics. 2023;65(5–6):384–396. DOI: 10.1007/s11141-023-10221-7.
30. Fliflet AW, Read ME. Use of weakly irregular waveguide theory to calculate eigenfrequ-

encies, Q values, and RF field functions for gyrotron oscillators. International Journal of Electronics Theoretical and Experimental. 1981;51(4):475–484. DOI: 10.1080/00207218108901350.
31. Borie E, Dumbrajs O. Calculation of eigenmodes of tapered gyrotron resonators // International Journal of Electronics. 1986;60(2):143–154. DOI: 10.1080/00207218608920768.
32. Sabchevski S, Idehara T, Saito T, Ogawa I, Mitsudo S, Tatematsu Y. Physical models and computer codes of the GYROSIM (GYROtron SIMulation) software package [Electronic resource]. FIR Center Report FIR FU-99. 2010. Available from:http://fir.u-fukui.ac.jp/FIR_FU99S.pdf.
33. Avramides KA, Pagonakis IG, Iatrou CT, Vomvoridis JL. EURIDICE: A code-package for gyrotron interaction simulations and cavity design. EPJ Web of Conferences. 2012;32:04016. DOI: 10.1051/epjconf/20123204016.
34. Melnikova MM, Rozhnev AG. Program for calculation of the eigenmodes electrodynamic parameter in the gyrotron with nonfixed field structure // Certificate of state registration of a computer program no. 2015615762, 22 May. 2015. (in Russian).
35. Bera A, Sinha AK. A novel approach for computation of high-order axial modes in a gyrotron resonator. IEEE Transactions on Electron Devices. 2018;65(12):5505–5510. DOI: 10.1109/TED. 2018.2877843.
36. Sawant A, Choi E. Development of the full package of gyrotron simulation code. Journal of the Korean Physical Society. 2018;73(11):1750–1759. DOI: 10.3938/jkps.73.1750.
37. Wang P, Chen X, Xiao H, Dumbrajs O, Qi X, Li L. GYROCOMPU: Toolbox designed for the analysis of gyrotron resonators. IEEE Transactions on Plasma Science. 2020;48(9):3007–3016. DOI: 10.1109/TPS.2020.3013299.
38. Semenov E, Zapevalov V, Zuev A. Methods for Simulation the nonlinear dynamics of gyrotrons. In: Balandin D, Barkalov K, Gergel V, Meyerov I. (eds). Mathematical Modeling and Supercomputer Technologies. MMST 2020. Communications in Computer and Information Science. Vol. 1413. Springer. 2021. P. 49–62. DOI: 10.1007/978-3-030-78759-2_4.
39. Vainshtein LA. Open Resonators and Open Waveguides. Golem Press; 1969. 439 p.
40. Vlasov SN, Zhisllin GM, Orlova IM, Petelin MI, Rogacheva GG. Irregular waveguides as open resonators. Radiophysics and Quantum Electronics. 1969;12(8):972–978.
41. Vlasov CN, Orlova IM, Petelin MI. Gyrotron cavities and electodynamic mode selection. In: Gaponov-Grekhov AV, editor. Gyrotron. Gorky, USSR: Inst. Appl. Phys. Acad. Sci. USSR; 1981:62–76 (in Russian).
42. Chu KR, Kou CS, Chen JM, Tsai YC, Cheng C, Bor SS, Chang LH. Spectral domain analysis of open cavities. International Journal of Infrared and Millimeter Waves. 1992;13(10):1571–1598. DOI: 10.1007/BF01009236.
43. Hung CL, Tsai YC, Chu KR. A study of open-end cavities by the field-energy method. IEEE Transactions on Plasma Science. 1998;26(3):931–939 DOI: 10.1109/27.700874.
44. Hung CL, Yeh YS. Spectral domain analysis of coaxial cavities. International Journal of Infrared and Millimeter Waves. 2003;24(12):2025–2041. DOI: 10.1023/B:IJIM.0000009758.76835.1f.
45. Sabchevski SP, Idehara T. A numerical study on finite-bandwidth resonances of high-order axial modes (HOAM) in a gyrotron cavity. Journal of Infrared, Millimeter, and Terahertz Waves. 2015;36(7):628–653. DOI: 10.1007/s10762-015-0161-9.
46. Genoud J, Tran TM, Alberti S, Braunmueller F, Hogge J-Ph, Tran MQ, Guss WC, Temkin RJ. Novel linear analysis for a gyrotron oscillator based on a spectral approach. Physics

of Plasmas. 2016;2(4):043101. DOI: doi.org/10.1063/1.4945611.
47. Ilínskiĭ AS, Slepyan GYa. Oscillations and waves in a electordynamic structures with losses. Moscow: Moscow State University; 1983. 232 p. (in Russian).
48. Genoud J, Alberti S, Tran TM, Le Bars G, Kaminski P, Hogge JP, Avramidis KA, Tran MQ. Parasitic oscillations in smooth-wall circular symmetric gyrotron beam ducts. Journal of Infrared, Millimeter, and Terahertz Waves. 2019;40(2):131–149. DOI: 10.1063/1.4945611.
49. Chu KR, Chen HY, Hung CL, Chang TH, Barnett LR, Chen SH, Yang TT, Dialetis DJ. Theory and experiment of ultrahigh-gain gyrotron traveling wave amplifier. IEEE Transactions on Plasma Science. 1999;27(2):391–404. DOI: 10.1109/27.772266.
50. Parlett BN. The Symmetric Eigenvalue Problem. First ed. NJ, USA: Prentice-Hall, Englewood Cliffs; 1980. 368 p.
51. Demmel JW. Applied Numerical Linear Algebra. Ca, USA: University of California; 1997. 419 p.
52. Golub GH, Van Loan CF Matrix Computations. 3th ed. Baltimore & London: John Hopkins University Press; 1996. 694 p.
53. Lehoucq RB, Sorensen DC, Yang C. ARPACK users' guide: solution of large-scale eigenvalue problems with implicitly restarted Arnoldi methods. Society for Industrial and Applied Mathematics. 1997.
54. Petelin MI, Yulpatov VK. Linear theory of a monotron cyclotron-resonance maser. I. Radiophys Quantum Electron. 1975;18(2):212–219. DOI: doi.org/10.1007/BF01036881.
55. Petelin MI. Self-excitation of oscillations in a gyrotron. In: Gaponov-Grekhov AV, editor. Collected papers. Gorki: Inst. Appl. Phys. USSR Academy of Science; 1981. P. 5–25.
56. Borie E, Jodicke B. Comments on the Linear Theory of the Gyrotron. IEEE Transaction on Plasma Science. 1988;16(2):116–121. DOI: 10.1109/27.3802.
57. Rozhnev AG, Adilova AB, Grigorieva NV, Ryskin NM. A program for calculating the properties of axial oscillation modes in an open gyrotron cavity by the finite difference method with boundary conditions linearized in the spectral parameter («GyrotronCavityFDM»). Certificate of state registration of a computer program № 2033613828, 09 May, 2023 (in Russian).
58. Yamaguchi Y, Tatematsu Y, Saito T, Kuwahara T, Ikeda R, Ogawa I, Idehara T, Dumbrajs O. Experimental verification of a self-consistent calculation for continuous frequency-tune with a 400 GHz band second harmonic gyro-BWO. In: Proceedings of the 38th Int. Conf. on Infr., Mill. and Terahertz Waves (IRMMW-THz). 01-06 September 2013, Mainz, Germany. New York: IEEE; 2013. P. 1–2. DOI: 10.1109/IRMMW-THz.2013.6665445.
59. Kumar A, Kumar N, Singh U, Khatun H, Vyas V, Sinha AK. Design of interaction cavity of a 170-GHz, 1-MW gyrotron for ECRH application. Vacuum. 2011;86(2):184–188. DOI: 10.1016/ j.vacuum.2011.06.002.
60. Thumm M. Effective cavity length of gyrotrons. Journal of Infrared, Millimeter, and Terahertz Waves. 2014;35(12):1011–1017. DOI: doi.org/10.1007/s10762-014-0102-z.
61. Hairer E, Wanner G. Solving Ordinary Differential Equations II. Stiff and Differencial-Algebraic Problems. Second Revised ed. Berlin: Springer-Verlag; 1996. 614 p.